JHEP PROCEEDINGS

Heavy Flavours 8, Southampton, UK, 1999

First measurement of $\mathrm{Re}(\varepsilon'/\varepsilon)$ from NA48

P. Lubrano

INFN Sezione di Perugia, Via A. Pascoli, Perugia, I-06100

E-mail: Pasquale.Lubrano@pg.infn.it

ABSTRACT: The NA48 detector has been collecting data to measure direct CP violation in the K^0 system since 1997. In this article we present the first result on the measurement of $\mathrm{Re}(\varepsilon'/\varepsilon)$ using data collected during the 1997 data-taking period, that is about 10% of the final sample that NA48 is expected to collect.

1. Introduction

Neutral Kaon decays have been, thus far, the only laboratory where Nature has manifested asymmetry between matter and antimatter. The "indirect" violation of the Charge and Parity symmetries (CP) in K meson decays has been firmly established since 1964, when unambiguous experimental evidence was reported[1]. The Standard Model also predicts "direct" CP violation, $\Delta S = 1$ transitions, dominated by the strong and electromagnetic penguin diagrams. "Indirect" CP violation leads to small branching fractions: theoretical predictions for "direct" CP[2] violation are difficult to make because of the lack of knowledge on the CKM matrix elements and uncertainties in calculating the contribution of the hadronic penguin diagrams. It should be stressed that alternative models[3], insisting on the $\Delta S = 2$ nature of a superweak interaction responsible for CP violation, do not contemplate the existence of "direct" CP violation.

Experimentally, "direct" CP violation can be inferred by observing a departure from unity of the ratio of branching fractions for neutral and charged kaon decays R, where R is defined as

$$R = \frac{\Gamma(K_L\to\pi^0\pi^0)}{\Gamma(K_S\to\pi^0\pi^0)} \cdot \frac{\Gamma(K_S\to\pi^+\pi^-)}{\Gamma(K_L\to\pi^+\pi^-)} \simeq 1 - 6\,\mathrm{Re}(\varepsilon'/\varepsilon)$$

and ε and ε' are the contributions from "indirect" and "direct" CP violation.

This method proves to be very powerful as many systematic uncertainties, which contribute simmetrically to the double ratio, can be controlled to high accuracy.

2. The NA48 Beam and Detector

The aim of the NA48[6] experiment is to measure the real part of ε' with an accuracy of 10^{-4}. The dominant source of errors are easily identified: 1) the statistics of $\Gamma(K_L \to \pi^0\pi^0)$ decays (by far the less abundant decay); 2) different energy scales for the reconstructed energies of charged and neutral events; 3) residual background in K_L decays; 4) accidental activities in the detector for K_L and K_S decays.K_L and K_S decays are provided by two nearly collinear and simultaneous beams, converging in the same region of the detector.

The layout of the beam line[7] is shown in Figure 1. A high intensity ($\sim 1.5 \times 10^{12}$ ppp) primary 450 GeV/c proton beam is used to produce the K_L beam at a small angle. After a first collimator, the protons emerging from the target are deflected onto a single bent crystal [9] that deviates a fraction of the protons producing a secondary proton beam which, after going through a tagging detector, is transported back on the beam line to the K_S target.

The fiducial decay region is defined as a length of of ≈15m (3.5 K_S lifetimes) from the beginning of the decay region which is precisely defined by a counter (AKS) in the K_S beam which vetoes all kaon decays upstream. The upstream end of the decay region for K_L and the downstream ends

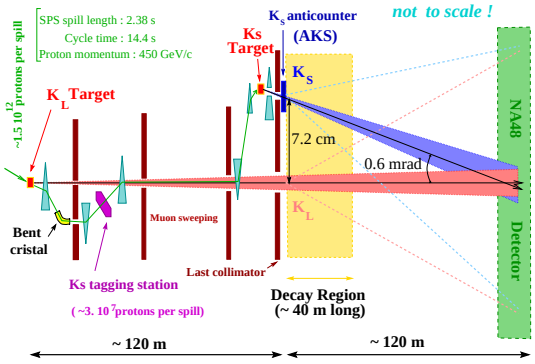

Figure 1: The neutral kaon beams layout.

for both are defined by a cut in the reconstructed longitudinal decay vertices.

In order to compensate for the naturally very different decay vertex distributions of K_L and K_S a weighting technique is used. Each K_L decay is weighted according to its longitudinal position, such that K_S and weighted K_L decay vertex distributions are made similar and their energy distributions agrees within $\pm 10\%$ over the accepted kaon energy range of $70 \leq E_k \leq 170$ GeV.

Events reconstructed in the charged or neutral spectrometer are assigned to K_L or K_S by comparing the time between the passage of a proton in the tagging counter and the event time as measured in the detector.

The tagging counter consists of two sets (horizontal and vertical) of 12 staggered scintillator counters, fixed on a high precision carbon fiber structure and each read out by a photomultiplier. The pulse height is sampled by 1 GHz FADC and the time of a charged particle can be measured with a time resolution better than 200 ps [8], while the two pulse separation is 4 nsec.

Figure 2 shows a schematic view of the NA48 detector downstream the K_S anticounter. The solid angle outside the detector acceptance is covered by rings of scintillator counters (seven).

The momenta of charged particles are measured in a magnetic spectrometer consisting of four planes of drift chambers and a central dipole magnet. The field integral is equivalent to a transverse momentum change of 265 MeV/c. The spatial resolution of the drift chambers, 100 μm, yields $\Delta p/p = 0.6\%$, while the resolution for the invariant K^0 mass is about 2.5 MeV/c.

The charged hodoscope, 64 scintillator counters arranged in two (vertical and horizontal) planes, serves a two fold purpose. It is used to provide a fast trigger on charged decays and to measure the time of charged events with a precision better than 200 ps (for single tracks).

They are followed by the liquid krypton (LKr) eletromagnetic calorimeter, whose construction has turned out to be a formidable task because of the stringent requirements imposed on the performances: high rate capability, excellent energy resolution, good position resolution and double photon separation. Furthermore, the calorimeter measures the time of neutral events with a precision comparable to what achieved for the charged ones. To achieve these goals a quasi–

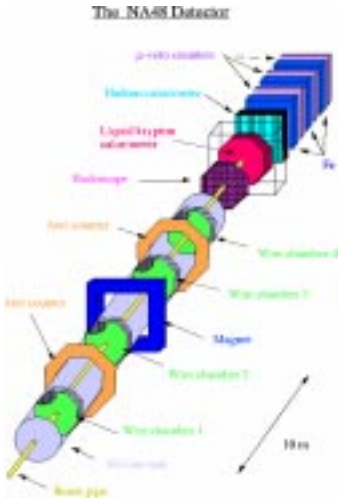

Figure 2: Schematic view of the NA48 detector.

homogeneous LKr electromagnetic calorimeter has been developed consisting of 2x2 cm^2 cells with a tower read out structure (the towers are parallel to the beam direction). The use of quasi–homogeneous liquid krypton as converter minimizes shower sampling fluctuations. The active volume is an octagon of 2.6 m width and 1.2 m depth (corresponding to $27X_0$) immersed in 8 m^3 of liquid krypton. The 13500 read out channels are read out by cold preamplifiers. Initial current read out technique, with a pulse shaping of 100 ns FWHM, is used and all pulses are digitized with

a 40 MHz FADC[10]. During the 1997 data taking period, due to a problem with the HV blocking capacitors, the calorimeter was operated at reduced electric field value (1.5 KV/cm): this resulted in a 20% worse signal to noise ratio with respect to the expected value. Due to a problem during the cooling phase a calorimeter column (4 cm wide) was not connected to HV, resulting in a 20% loss in $K^0 \to \pi^0\pi^0$ events.

The energy resolution is $\sigma_E/E = [(0.125/E)^2 + 0.032^2/E + 0.005^2]^{1/2}$ where E is measured in GeV. The space resolution is better than 1.3 mm in both x and y directions (above 20 GeV) and the time resolution is better than 300 ps for 20 GeV electromagnetic showers.

A second time measurement for neutral events is performed by a scintillating fiber hodoscope (neutral hodoscope) placed at $10X_0$ inside the LKr calorimeter. The neutral hodoscope is made up by ∼20 Km of scintillating fibers arranged in fiber bundles and read out by 32 photomultipliers. Both fibers and photomultipliers are completely contained in the liquid krypton (T = 120°K). This device also provides an independent trigger for neutral decays.

Muon detection is accomplished using a set of three planes of scintillator counters separated by 80 cm of iron. Together with a lead–scintillator sandwich hadron calorimeter and the magnetic spectrometer, they are used to reject the background due to the charged semileptonic K_L decays.

In order to cope with the high intensity a two-level charged trigger[12] selected $K^0 \to \pi^+\pi^-$ events. The first level was accomplished by a coincidence between a total energy condition (>30 GeV) and a charged hodoscope coplanarity configuration (Q_x) and, after being downscaled by a factor of 2, triggered the second level. This uses information from drift chamber hits and consists of a processors farm: starting from space points, the farm reconstructs charged tracks, their invariant mass and decay vertex position.

The neutral trigger[11] is based solely on the digitized calorimeter information. The calorimeter data are reduced to X and Y projections and events are selected based on total energy, number of peaks in each projection, center of gravity and reconstructed proper decay time.

3. Event reconstruction and selection

All events are required to satisfy some common fiducial cuts on energy range and proper time, namely $70 < E_K < 170$ GeV and $0 < \tau < 3.5$, τ=0 being defined by the position of the AKS counter. For K_S decays the τ=0 cut is defined naturally by the AKS which vetoes all decays upstream, while the remaining constraints are imposed on the reconstructed quantities.

Data collected in the charged mode are affected by an overflow condition in the drift chambers occurring by accidental particles showering upstream of the sprectrometer. In the analysis, events were required not to have an overflow condition within ±312 nsec of the trigger time. To reduce possible biases, this selection is applied to neutral events as well, resulting in a 20% loss of statistic.

3.1 Charged events

$K^0 \to \pi^+\pi^-$ events are reconstructed in the magnetic spectrometer, starting from drift chamber space points. The momenta of the tracks are derived by their curvature in the magnetic field (for which a detailed field map is used). The decay vertex is defined as the point of closest approach of the two oppositely charged tracks: the resolution with which it is measured is tipically 50 cm in the longitudinal direction (Z) and 2 mm in the transverse plane.

A momentum dependent cut on the variable $A = |p_1 - p_2|/|p_1 + p_2|$ ($A < 0.62 \text{and} A < 1.08 - 0.0052 \times E_k$) eliminates asymmetric events with tracks near the beam line and Λ decays coming from the K_S beam.

Semileptonic decays ($K_\mu 3$ and $K_e 3$) are rejected by identifying the muons using the muon detector and electrons by comparing the energy deposited in the electromagnetic calorimeter with the momentum measured in the charged sprectrometer ($E/p < 0.8$). These decays are reduced by a factor of 500, whereas they are highly efficient for real $\pi^+\pi^-$ decays. A cut on a transverse momentum variable further reduced background from semileptonic decays. A selection which is symmetric in between K_S and K_L is accomplished by defining a variable p'_T as the component of the kaon momentum perpendicu-

lar to the line joining the production target and the point where the kaon trajectory crosses the plane of the first drift chamber.

Finally, for good charged decays the invariant mass of the oppositely charged tracks should be consistent with the known kaon mass. A momentum dependent cut of $\pm 3\sigma$ ($\sigma = 2.5 MeV/c^2$) is used.

The event time, used by the tagging method to discriminate between K_S and K_L, is obtained by combining the 4 times obtained by the two charged hodoscope planes for the two tracks.

3.2 Neutral events

$K^0 \to \pi^0\pi^0$ events are reconstructed by requiring the presence of four photon showers in the electromagnetic calorimeter. Fiducial cuts are applied to ensure that the energy of the photons is well measured: photon candidates should be at least 2 cm away from any dead cell and from the dead column, the minimum distance in between two photon candidates should exceed 10 cm.

Photon energies are obtained by looking for maxima in the digitized pulses and summing the energy deposited in a window of 11 cm radius. Each photon is required to have energy in between 3 and 100 GeV and a time consistent (within $\pm 5 nsec$) with the weighted average of the four. Events containing an additional shower in excess of 1.5 GeV and within $\pm 3 nsec$ of the average are rejected.

The longitudinal position of the decay vertex, with respect to the front of the calorimeter, is reconstructed from the energies and impact points (assuming the kaon invariant mass) of the four photon candidates using

$$D = \sqrt{\sum_i \sum_{j>i} E_i E_j d_{ij}^2}/m_K$$

where $d_{ij}^2 = (x_i - x_j)^2 + (y_i - y_j)^2$. The invariant masses, m_1 and m_2, of the two photon pairs are computed using D and compared to the known π^0 mass to form a χ^2 variable, defined as

$$\chi^2 = [\tfrac{(m_+ - m_{\pi^0})}{\sigma_+}]^2 + [\tfrac{m_-}{\sigma_-}]^2$$

where $\sigma_\pm$ are the resolutions of $m_\pm = (m_1 \pm m_2)/2$ observed in the data. Of the three possible photon pairings the one resulting in the lowest χ^2 is selected, and to select $K^0 \to \pi^0\pi^0$ candidates the best combination is required to have $\chi^2 < 13.5$

The event time for neutral decays is measured using 8 time measurements from the two most energetic cells of each of the four photon showers of the candidate event.

3.3 Tagging

Events are tagged as K_S or K_L based upon the presence of a proton in the tagger detector in coincidence with the time of the event. Events having a proton in coincidence, within a window of $\pm 2 nsec$ centered around the event time, are tagged as K_S and, otherwise, as K_L.

This tagging method results in transition probabilities (L $\to$ S and S $\to$ L) which have to be known precisely in order not to contribute significantly to the sistematic error. The presence of an accidental proton in the tagger in coincidence with a K_L decay causes the event to be wrongly counted as K_S (α_{LS} transition probability), whereas any inefficiency in the tagger detector or time measurement error for the event would result in a K_S event to be wrongly counted as K_L (α_{SL} transition probability).

The double ratio R is sensitive to any difference in these probabilites between $\pi^0\pi^0$ and $\pi^+\pi^-$ events. These transitition probabilities are precisely measured for charged decays by identifying K_S or K_L using their reconstructed vertex position, as the two beams are about 7 cm apart in the Y direction. The corresponding probabilites for neutral events (or their difference with respect to charged ones) are measured using samples of neutral events containing π^0 Dalitz decays and photon conversions and $3\pi^0 K_L$ decays (α_{SL} or by looking at proton coincidences in the sidebands of the actual event (α_{LS}), The results of these studies show that $\alpha_{LS}^{00} - \alpha_{LS}^{+-} = (10 \pm 5) \times 10^{-4}$, which translates into a correction for the double ratio R of $(18 \pm 9) \times 10^{-4}$, and $\alpha_{SL}^{00} - \alpha_{SL}^{+-} = (0 \pm 1) \times 10^{-4}$, resulting in an uncertainty on R of $\pm 6 \times 10^{-4}$.

3.4 Final samples

The final samples, after correcting for event mistagging and background subtraction, without lifetime correction, are shown in Table 1.

Decay mode	No. of events (K)
$K_L \to \pi^0\pi^0$	489
$K_S \to \pi^0\pi^0$	975
$K_L \to \pi^+\pi^-$	1071
$K_S \to \pi^+\pi^-$	2087

Table 1: Statistical samples (thousands of events).

4. Background and corrections

In this section we discuss the background subtraction and corrections to the double ratio R. Only the most important sources of systematic errors will be considered here, for a more comprehensive treatment of the different sources and their effect on the measurement of R the reader should refer to [13]. All of the following corrections are applied bin by bin over the fiducial energy range, although the values reported here are their averages over the interval 70–170 GeV.

The correction introduced by mistagging have already been discussed individually in the Tagging section. Their collective effect is $(+18 \pm 11) \times 10^{-4}$

The neutral trigger efficiency is measured using events triggered only by the scintillating fiber detector (neutral hodoscope) and it is found to be 0.9988 ± 0.0004 for both K_S and K_L. The charged trigger efficiency is measured, using a set of events triggered by auxiliary triggers, to be 0.9168 ± 0.0009. A small difference for the detection efficiency of $K_S \to \pi^+\pi^-$ and lifetime weighted $K_L \to \pi^+\pi^-$ events, introduces a correction of $(+9 \pm 23) \times 10^{-4}$. Most of the uncertainty here is due to the lack of statistics in the control sample used to measure the efficiency due to a high downscaling factor used in the auxiliary trigger. This was corrected after 1997.

The acceptance for K_S and K_L events are made similar by weighting K_L events according to their proper decay time, so that their effective decay vertex distribution is very similar to the K_S one. Residual differences are studied using a complete simulation of the beams and detector. Uncertainties in the positions and divergences of the beams are responsible for the major component of the systematic error in the acceptance correction. The dead column, present in the 1997 run, also contributes to the acceptance correction to the double ratio which is $(29 \pm 11(MCstat) \pm 6(syst)$.

Neutral events are reconstructed using photon energies in the calorimeter. The measured kaon energy, decay vertex and proper time are affected by how well the individual photon energies are measured. The calorimeter performances have been studied using neutral $\pi^0\pi^0$, semileptonic K_{e3} decays and special runs were a negative pion beam produced η mesons by impacting on a special target placed near the AKS counter. The overall energy scale is adjusted using $K_S \to \pi^0\pi^0$ events: the beginning of fiducial region being defined by the AKS counter which vetoes upstream decays. A continuous monitoring of the energy scale showed its stability within $\pm 5 \times 10^{-4}$ over the entire run, resulting in a correction term of $(0 \pm 5) \times 10^{-4}$ on R. The uniformity of the calorimeter and non linearities were studied using K_{e3} decays and their corresponding correction to the double ratio is $(0 \pm 3) \times 10^{-4}$ and $(0 \pm 9) \times 10^{-4}$. Taking into account uncertainties on the correction of individual photon energies (energy sharing, space charge effects...) and summing in quadrature all the above effects, the overal correction to the double ratio is found to be $(0 \pm 12) \times 10^{-4}$

Finally, the effect of accidental activity in the detector is minimized by the technique of collecting all four decays modes concurrently. The residual effects are arising mostly from K_L decays or from particles originating from the K_L target. These are studied by overlaying randomly triggered events to real ones: this method provides a measurement of intensity effects in terms of gains and losses. The effect on the double ratio is small and the resulting correction is $(-2 \pm 14) \times 10^{-4}$, where the uncertainty is dominated by the lack of statistic of the sample of events used for the overlay analysis.

5. R result

The individual contribution to the systematic error for the double ratio R, discussed in the previous section, are summarized in Table 2.

It should be stressed that the most relevant systematic errors suffer from lack of statistical power in the analysis, and therefore one would

Source	Correction to R
Tagging	$+18 \pm 11$
Charged trigger	$+9 \pm 23$
Acceptance	$+29 \pm 12$
Accidentals	-2 ± 14
Neutral Background	-8 ± 2
Charged Background	$+23 \pm 4$
Scattering	-12 ± 3
Energy scale	0 ± 12
Charged Vertex	0 ± 5

Table 2: Corrections to R (in 10^{-4} units.)

expect better precision once the final statistical sample will be available.

The double ratio R is computed in 20 energy bins between 70 and 170 GeV. Corrections are applied bin by bin, and the final result is shown in Figure 3. Also shown as open circles are three additional points, measured outside the boundaries of the fiducial energy region. Although these points provide additional robusteness to the result, especially when assessing the possibility of a linear energy trend of the data, they have not been used in the fit to the determine the final value of the double ratio.

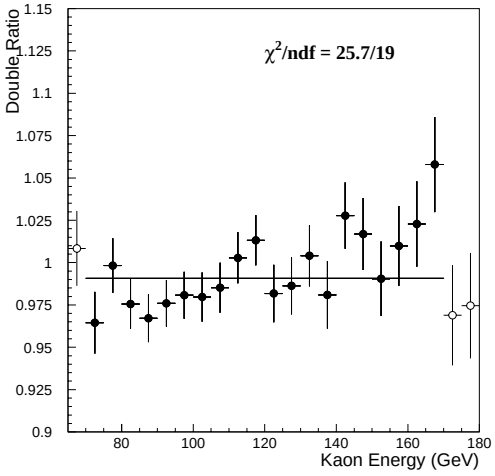

Figure 3: The double ratio R, in energy bins, between 70 and 170 GeV.

The χ^2 of a fit to a constant value is 25.7 for 19 degrees of freedom. Extensive checks have been carried out to exclude biases which could lead to an energy dependence in our calculation of R. The final result for R is $0.9889 \pm 0.0027 \pm 0.0035$, where the first error is due to statistics and the second is systematic. The corresponding value for the direct CP violating parameter is

$$\mathrm{Re}(\varepsilon'/\varepsilon) \quad (18.5 \pm 4.5 \pm 5.8) \times 10^{-4}$$

or, summing the statistical and systematic error in quadrature,

$$\mathrm{Re}(\varepsilon'/\varepsilon) \quad (18.5 \pm 7.3) \times 10^{-4}$$

Figure 4 shows this measurement (together with previous results obtained at CERN and FNAL and the most recent measurement of FNAL) compared to several theoretical estimates for $\mathrm{Re}(\varepsilon'/\varepsilon)$. The yellow band is centered at the new world average value and its width is given by the experimental error. The four red points are four recent theoretical estimates: they fail to reproduce the experimental results.

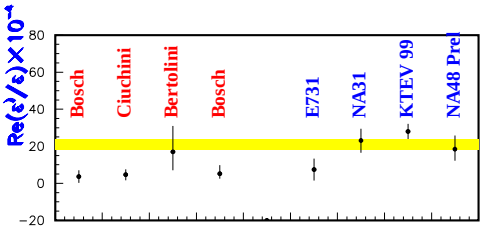

Figure 4: R measurements versus theory.

6. Conclusions

Using data collected during the 1997 data period, which corresponds to 10% of the expected total NA48 sample, we have measured $\mathrm{Re}(\varepsilon'/\varepsilon) = (18.5 \pm 4.5 \pm 5.8) \times 10^{-4}$. This result clearly favours a non zero value for $\mathrm{Re}(\varepsilon'/\varepsilon)$. The KTeV collaboration has recently measured $\mathrm{Re}(\varepsilon'/\varepsilon) =$

$(28.0 \pm 4.1) \times 10^{-4}$[14] using about 25% of their expected final sata sample.

Further improvements in the NA48 data acquisition system and read-out electronics have allowed during 1998 and 1999 to collect more data for which the analysis is well underway.

References

[1] J. H. Christensen, J. W. Cronin, V. L. Fitch and R. Turlay, Phys. Rev. Lett. 13 (1964) 138.

[2] A. Buras et al., Phys. Lett. B389 (1996) 749;
M. Ciuchini et al., Phys. Lett. B301 (1993) 263;
M. Ciuchini et al., Z. Phys C68 (1995) 239;
S. Bertolini et al., Nucl. Phys. B476 (1996) 225.

[3] L. Wolfenstein, Phys. Rev. Lett. 13 (1964) 562.

[4] G.D.Barr et al.: Phys. Lett. B317 (1993) 233.

[5] L.K.Gibbons et al.: Phys. Rev. Lett. 70 (1993) 1203.

[6] G.D. Barr et al., CERN/SPSC/90-22 and CERN/SPSLC 91-58.

[7] C Biino et al., CERN-SL-98-033 (EA).

[8] P. Grafstrom et al., Nucl. Instr. and Methods A344 (1994) 487;
H. Bergauer et al, NUcl. Instr and Methods A419 (1998) 623.

[9] N.Doble et al., Nucl. Instr. and Methods, B119 (1996) 181.

[10] B. Halgren et al., Nucl. Instr and Methods, A419 (1998) 680.

[11] B. Gorini et al., IEEE Trans. Nucl. Sci. 45 (1998) 1771.

[12] S. Anvar et al., Nucl. Instr and Methods, A419 (1998) 686.

[13] V. Fanti et al., CERN-EP/99-114, submitted to Phys. Lett. B.

[14] A. Alavi-Harati et al., Phys. Rev. Lett. 83 (1999) 22.